HHS Public Access

Author manuscript

Measurement (Lond). Author manuscript; available in PMC 2016 January 29.

Published in final edited form as:

Measurement (Lond). 2015 September ; 73: 318–334. doi:10.1016/j.measurement.2015.05.039.

An examination of an adapter method for measuring the vibration transmitted to the human arms

Xueyan S. Xu*, **Ren G. Dong**, **Daniel E. Welcome**, **Christopher Warren**, and **Thomas W. McDowell**

Engineering & Control Technology Branch, National Institute for Occupational Safety and Health, 1095 Willowdale Road, Morgantown, WV 26505, USA

Abstract

The objective of this study is to evaluate an adapter method for measuring the vibration on the human arms. Four instrumented adapters with different weights were used to measure the vibration transmitted to the wrist, forearm, and upper arm of each subject. Each adapter was attached at each location on the subjects using an elastic cloth wrap. Two laser vibrometers were also used to measure the transmitted vibration at each location to evaluate the validity of the adapter method. The apparent mass at the palm of the hand along the forearm direction was also measured to enhance the evaluation. This study found that the adapter and laser-measured transmissibility spectra were comparable with some systematic differences. While increasing the adapter mass reduced the resonant frequency at the measurement location, increasing the tightness of the adapter attachment increased the resonant frequency. However, the use of lightweight (≤15 g) adapters under medium attachment tightness did not change the basic trends of the transmissibility spectrum. The resonant features observed in the transmissibility spectra were also correlated with those observed in the apparent mass spectra. Because the local coordinate systems of the adapters may be significantly misaligned relative to the global coordinates of the vibration test systems, large errors were observed for the adapter-measured transmissibility in some individual orthogonal directions. This study, however, also demonstrated that the misalignment issue can be resolved by either using the total vibration transmissibility or by measuring the misalignment angles to correct the errors. Therefore, the adapter method is acceptable for understanding the basic characteristics of the vibration transmission in the human arms, and the adapter-measured data are acceptable for approximately modeling the system.

Keywords

Hand; arm vibration; Hand-transmitted vibration; Human vibration measurement; Vibration dosimeter; Adapter method

*Corresponding author at: ECTB/HELD/NIOSH/CDC, 1095 Willowdale Road, MS L-2027, Morgantown, WV 26505, USA. Tel.: +1 (304) 285 5840; fax: +1 (304) 285 6265. XueyanXu@cdc.gov (X.S. Xu).

Disclaimers

The content of this publication does not necessarily reflect the views or policies of the National Institute for Occupational Safety and Health (NIOSH), nor does mention of trade names, commercial products, or organizations imply endorsement by the U.S. Government.

1. Introduction

Prolonged, intensive exposure to hand-transmitted vibration may cause a range of effects and health problems [1–3]. Vibration biodynamics are a major foundation for understanding the mechanisms of the vibration effects and for developing anti-vibration devices [4,5]. It has been hypothesized and partially proven that the biodynamic responses such as vibration forces, stresses, strains, and power absorbed and dissipated in the system are closely associated with vibration-induced injuries and dysfunctions of the tissues or biological structures of the system [5–11]. However, while these biodynamic responses can be measured on cadavers [12], no *in vivo* technology is available to directly measure the responses inside the substructures of a live human subject. Alternatively, biodynamic responses can be predicted using computer models [10,13,14]. The directly-measurable biodynamic response functions such as vibration transmissibility on the skin of the hand–arm system and/or driving-point biodynamic response functions have been widely used to calibrate such models [10,13–19], as the measured response functions reflect the overall biodynamic properties of the system and have certain relationships with the internal biodynamic responses [20]. The vibrations measured at wrist, elbow, and shoulder may also be directly used to assess the vibration-induced disorders and injuries in these joints, similar to the method for assessing the shock-induced health effects in the human lumbar spine recommended in ISO 2631-5 [21]. The theoretical basis of this method is that the dynamic forces, stresses, and strains at these locations are likely to be highly correlated with the vibrations measured at these locations. For this reason, the vibration transmissibility can also be used to help develop location-specific frequency weightings for assessing the risk of vibration exposure [11,22,23]. Vibration transmissibility can also be used to evaluate the effectiveness of anti-vibration devices and the improvement of powered hand tools [24]. Therefore, the measurement of the transmitted vibrations remains one of the important tasks for further studies of hand-transmitted vibration exposures and health effects.

It is conventionally assumed that the transmissibility of a substructure should be measured on a bony anatomy [25]. This is consistent with the hypothesis that the vibration is primarily transmitted through the bones and joints of the human body. However, this assumption is not fully suitable for studying human vibration exposures, especially hand-transmitted vibration exposures. First, the bone vibration is unlikely to be directly related to the major components of the hand–arm vibration syndrome (HAVS), as they are primarily associated with soft tissue injuries and disorders [1–3,26]. Second, the bone mass is usually less than 20% of the total mass of the human body [27]; the bone vibration is unlikely to be representative of the overall motion of the substructure. This is also because the bone and its surrounding soft tissues may vibrate largely differently at some frequencies in the major frequency range (5–1500 Hz) of concern [26]. Ideally, the transfer functions of the bones and soft tissues should both be measured for the synthesis of the representative transmissibility of each substructure or for the separate simulations of the hard and soft tissues [20]. Unfortunately, no *in vivo* technology has been developed to perform the measurement on the bones. The model development has to depend primarily on the transmissibility measured on skin surface and other measurable information. Although this makes the model development more difficult, it is theoretically feasible [28]. A

comprehensive understanding of the surface transmissibility measurement may provide improved applications of the measured data for the model development.

Many studies have investigated the surface vibration transmissibility of the hand–arm system [29–39]. There are considerable differences among the reported data [37]. Some of the differences reflect the natural characteristics of the hand–arm biodynamic responses to vibration and are functions of influencing factors such as vibration frequency, direction, magnitude, location on the system, hand and arm postures, applied hand forces, and individual differences. The other differences are likely to be associated with the measurement methods [37]. The majority of the reported studies used miniature accelerometers in the measurement. The attachment of the accelerometer on the skin may change the local dynamic properties of the hand–arm system, and the measurement may thus be affected by the mass of the accelerometer and fixture, as well as the attachment tightness. The accelerometer may also vibrate rotationally on the deformable skin base, which may also affect the measurements of the transmitted vibrations. A tight attachment may reduce the rotational effect and make the measurement more representative of the bone response, especially at a bony location. However, a tight attachment is not desired when the soft tissue transmissibility is of interest, especially in the non-bony areas with thick layers of soft tissue. Furthermore, a tight attachment may cause subject discomfort, as a tight attachment may apply large stresses on the soft tissues and largely constrain the blood flow in the hand–arm system. Although these factors are generally recognized, no comprehensive investigations of their effects on the measurement have been reported. Such knowledge is required to appropriately apply the conventional accelerometer for the measurement of the transmissibility. Furthermore, the local coordinate systems of the accelerometers attached to the skin may be different from the global coordinate systems of the excitations, which may also vary with the measurement location, hand and arm postures, individual differences, attachment forces etc. It is unclear whether these possible measurement errors are within the acceptable range for the transmissibility applications. Moreover, no proven techniques for reducing the effects of such measurement errors have been established.

When the skin surface transmissibility is of interest, the sensor attachment issues can be avoided by using a laser vibrometer due to its non-contact measurement capabilities. While single-axis (1-D) laser vibrometers have been used in some studies [32,38–40], a three-dimension (3-D) laser vibrometer has also been recently used in a few other studies [41,42]. However, the laser vibrometers also have their own limitations. The hands and arms can displace over large ranges during tool operation; it is very difficult to use the laser vibrometer to measure the vibrations at workplaces. While it is not very difficult to focus the 1-D laser beam on the stationary hand or arm during a laboratory measurement, it can be a challenging task to focus the three laser beams on the same measuring point on the arms using a 3-D scanning laser vibrometer. As a result, the data measured from different trials may vary [41,42], although the differences may be partially attributed to the variations of the hand forces and postures. This observation suggests that the laser vibrometers are suitable for a stationary posture in a laboratory, but they may not provide more reliable measurement than conventional methods in other measurement conditions.

The development of a convenient, portable, robust, and reliable device for measuring and monitoring the vibrations transmitted to the human body at workplaces likely has to rely on the improvement of the conventional accelerometer method. Such a device is also highly desirable for conducting cost-effective experiments in many laboratory studies. This study hypothesizes that a lightweight instrumented adapter can serve as such a device. As a step toward the development of a portable device and the improvement of the adapter method, the objective of this study is to investigate the validity of the adapter method for measuring the vibrations transmitted to the human arms. Besides the measurement with the conventional method, two laser vibrometers are used to measure the vibrations transmitted to the skin at the wrist and on the arms. The laser-measured data are compared with those measured using the adapter method at the same locations, which is used to identify the influences of the adapter-accelerometer assembly and fixture on the transmissibility measurement. The apparent mass of the hand–arm system along the forearm direction is also measured in part of the experiments, which is used to help understand and evaluate the transmissibility data based on the theoretical relationship between the transmissibility and apparent mass identified in a recent study [20]. A model of the hand–arm system is also used in the evaluation. The implications of the experimental and theoretical results are discussed.

2. Methods

According to the reported experimental data [41,42], vibration at frequencies above 100 Hz is not effectively transmitted to the human arms. As powered hand tools do not usually generate substantial vibrations below 5 Hz, and the standard method for the exposure risk assessment focuses on frequencies above 5 Hz [26]. To verify the effective frequency range of the arm responses and to ensure the entire response frequency range is covered, this study considered the frequency range of 4–500 Hz for the transmissibility measurements. Because our current 3-D vibration test system cannot generate sufficient vibration below 10 Hz, we conducted two series of experiments on two vibration test systems to cover the frequency range. The first series was conducted on a 3-D vibration test system from 10 to 500 Hz. The second experiment was performed on a 1-D test system along the forearm direction from 4 to 400 Hz. The basic setups of the two experiments are similar, which are illustrated in Fig. 1. Different random vibration spectra were used in the experiments, which are plotted in Fig. 2. Six healthy male subjects participated in each experiment. Their major anthropometries are listed in Table 1. The study protocols were reviewed and approved by the NIOSH Human Subjects Review Board.

2.1. Adapters and accelerometers

Four adapters were fabricated using different materials based on the geometric design recommended in the standardized glove test [43], which are shown in Fig. 3(a). Adapter A was made of magnesium; Adapter B was made of wood; Adapter C was made of aluminum; and Adapter D was made of polylactic acid (PLA) using a 3-D printer. Each adapter was equipped with a tri-axial accelerometer (Endevco, M35A). The adapters A, B, C, and D with the accelerometers installed weigh 13 g, 15 g, 31 g, and 7 g, respectively. Initially, only Adapters A, B, and C were made and used in the 3-D experiment. As Adapter B performed the best in the 3-D test, it was selected for the follow-up 1-D experiment. To further

investigate the mass effect on the transmissibility measurement, the lightest adapter (Adapter D) was also made and used in the 1-D experiment.

2.2. The measurements on the 3-D vibration test system

2.2.1. Instrumentation and check-up test—The vibration excitations on the 3-D test system are provided by three 1-D shakers arranged in three orthogonal directions [44]. The vibration is delivered to the human hand through an instrumented handle that is connected with each shaker using a flexible linkage system so that the vibration in each direction can be realized using a vibration control system [44]. The instrumented handle is equipped with a tri-axial accelerometer (Endevco, 65–100) and a pair of force sensors (Interface, SML-50) for measuring the accelerations and applied grip force. A force plate (Kistler, 9286AA) was used to measure the push force applied to the handle. The applied and target grip and push forces were displayed on two virtual dial gauges on a computer monitor in front of the subject. Besides the 3-D vibrometer, Adapters A, B, and C described above and shown in Fig. 3(a) were used to measure the transmitted vibrations on the subjects' arms during the 3-D experiment.

To establish baseline transmissibility of the adapters, each adapter was firmly attached to the instrumented handle on the 3-D test system using rubber bands, as shown in Fig. 3(b). The vibration transmissibility spectra on the adapter were simultaneously measured using both the accelerometer and laser vibrometer. To further check the validity of the measurement and calculation method described in Section 2.4, a piece of foam (10 mm thick open-cell polyurethane foam) was inserted between the adapter and handle, as shown in Fig. 3(c). The foam enables the adapter to exhibit a significant resonant response in the tested frequency range, which can be used to check the consistency of the measurements using the laser vibrometers and accelerometers under resonant responses.

2.2.2. Subject test—The basic subject posture used in the experiment is illustrated in Fig. 1. A pictorial view of a subject holding the instrumented handle during the measurement is also shown in Fig. 4. The subject was instructed to grip the handle with the forearm parallel to the floor and aligned with the *Z* axis with the elbow angled between 90° and 120°; these postures were similar to those recommended in the standard glove test [43]. Also, as required in the standard glove test, the grip force was controlled within 30 ± 5 N and the push force within 50 ± 8 N.

To examine the adapter effect on skin vibration, the vibration transmissibility on the skin at each of the three locations (wrist, forearm, and upper arm) was measured using both the laser vibrometer and the adapters. The measurement using only the laser vibrometer is shown in Fig. 4(a); the measurement using the adapter method is shown in Fig. 4(b). The three adapters were attached to the three measurement locations using elastic cloth bands. To directly compare the vibrations measured using the two methods, the laser vibrometer measurement was performed simultaneously with the adapter measurements. To enhance laser measurement quality, retro-reflective tape was applied to each measurement point, which is also shown in Fig. 4.

To examine the effect of the tightness of the elastic cloth adapter attachment on the measurement, this study applied two levels of wrapping force on each adapter for the attachment: medium (4 ± 1 N) and tight (8 ± 1 N) attachments. Under the medium tightness level, the cloth's tension was just adequate to securely hold the adapter at the designed location during the measurement. A higher tension was applied for the tight level of attachment such that the subject was not uncomfortable and the cloth not too restrictive. The applied wrapping force was not directly measured on each subject. It was measured by simulating the attachment on the instrumented handle of the vibration test system. To simulate the elasticity of the arm, the same foam as used in the adapter baseline test was wrapped on the handle and the adapter was wrapped on the foam. To ensure that the attachment force was applied consistently, one researcher implemented the attachment using the elastic cloths in the simulation and for all adapters and subjects.

During the 3-D experiments, a trial consisted of a sequence whereby the 3-D laser vibrometer scanned each of the three measurement locations while acceleration data were simultaneously collected via the three adapters (Fig. 4(b)). After two trials with a particular adapter arrangement and tightening condition, the adapters were exchanged with one another to comprise a different adapter/location arrangement, and two more replicates were completed. This process was repeated until each of the three adapters was used for two trials at each of the three measurement locations and with the two attachment tightness levels (3 locations × 2 adapter tightening conditions 2 × replicates = 12 trials). Two additional trials were completed for the laser measurement on the skin without adapters (Fig. 4(a)). Thus, a total of 14 trials were completed for each subject. The order of the tests was independently randomized among the subjects. Each trial lasted about 20 s. The subject rested for more than one minute between trials.

2.3. The measurements on the 1-D vibration test system

After recognizing the limitations of the 3-D experiment, we conducted a further test on a 1-D test system to explore the resonance in the lower frequency range (<25 Hz) and to verify the 3-D experimental results. A pictorial view of the 1-D experiment is shown in Fig. 5. It was used to measure the transmissibility along the forearm direction (*Z* axis). Although the 1-D vibration test system is supposed to generate vibration only along the *Z* axis, it generates small vibrations in the other two orthogonal directions when the hand is coupled on the instrumented handle [45]. To account for the non-axial vibrations, the instrumented handle measured the input vibration using the tri-axial accelerometer installed in the handle. Adapters B (wood) and D (PLA) described in Section 2.1 above were used to measure the skin surface accelerations in the 1-D experiments. A 1-D laser vibrometer (Polytec PI, H300) was used to measure the vibration transmissibility of the upper arm in the forearm axial (*Z*) direction. Because the laser beam could not reach the measuring points on the forearm, it was not used for the measurement on the forearm and at the wrist. The instrumentation check-up test, subject postures, hand forces, and test procedures used in the 1-D experiments were the same as those used in the 3-D experiments, except that only two adapter measurement points were used (wrist and upper arm), and only the medium tightness level was used for the adapter attachment.

The apparent mass at the palm of the hand along the forearm direction was also simultaneously measured with the vibration transmissibility in the 1-D experiment using a method reported before [46]. Briefly, the dynamic force at the driving point was measured using the force sensors installed in the instrumented handle. The dynamic force, together with the acceleration measured on the measuring cap of the instrumented handle, was used to calculate the apparent mass. As the directly measured apparent mass includes the tare mass of the measuring cap, the actual apparent mass at the palm of the hand was obtained by subtracting the tare mass from the directly measured data [46].

2.4. Calculations of transmissibility

This study used the same concept as that used to compute glove vibration transmissibility in the standard glove test [43]. As the first step, the accelerations in each direction on the handle and the adapter attached to the handle are measured. The baseline transmissibility in each of the three directions was computed from

$$T_{i\_Adapter-Baseline}=\frac{A_{i\_Bare-Adapter}}{A_{i\_Handle}} \quad i=X,Y,Z \quad (1)$$

$$T_{i\_Laser-Baseline}=\frac{A_{i\_Bare-Laser}}{A_{i\_Handle}} \quad i=X,Y,Z \quad (2)$$

where A_{i_Handle} is the input acceleration in each direction measured with the tri-axial accelerometer installed in the handle; $A_{i\_Bare\text{-}Adapter}$ is the acceleration on the adapter attached to the handle; $A_{i\_Bare\text{-}Laser}$ is the acceleration on the adapter attached to the handle measured using the laser vibrometer or the acceleration on the handle surface measured with the laser vibrometer.

The baseline total vibration transmissibility measured with the adapter or laser was computed from

$$T_T\text{-}Baseline-j=\frac{\sqrt{A^2_{X\_Bare-j}+A^2_{Y\_Bare-j}+A^2_{Z\_Bare-j}}}{\sqrt{A^2_{X\_Handel}+A^2_{Y\_Handel}+A^2_{Z\_Handel}}} \quad (3)$$
$$j=Adapter, Laser$$

As the second step, the transmitted accelerations measured with the adapters and laser vibrometer, together with handle accelerations, were used to calculate the transmissibility for each subject ($T_{\text{-}Raw}$). Their formulas used for the calculation of the subject transmissibility are the same as Eqs. (1)–(3), except the transmitted accelerations are measured in the subject test.

As the third step, the corrected transmissibility (T) was calculated using the baseline transmissibility ($T_{\text{-}Baseline}$) from Step 1 and the directly-measured transmissibility ($T_{\text{-}Raw}$) from Step 2, which is expressed as follows:

$$T_{i\_j}=\frac{T_{i-Raw-j}}{T_{i-Baseline-j}};\ i=X,Y,Z,T;\ j=Adapter,Laser \quad (4)$$

2.5. Correction of adapter misalignment to global coordinate axes

The laser measurement is based on a global coordinate system aligned with the instrumented handle of the vibration test system. The adapter measurement, however, is based on a local coordinate system or the adapter coordinate system, which may vary with the measurement location on the human body. Therefore, the laser-measured and adapter-measured directional transmissibility results may not be directly comparable. Furthermore, the transmissibility in the global coordinate system is usually required in some applications such as the modeling of the hand–arm system and the investigation of vibration direction effects. To perform the coordinate system transformation, it is necessary to measure the angular positions of the accelerometer or adapter attached to the skin of the body. This is demonstrated in this study. As shown in Fig. 6, the *z* axis of the adapter attached to the wrist can be approximately aligned with the global *Z* axis, but the global *X* and *Y* coordinates are not naturally aligned with the local *x* and *y* axes for the hand and arm postures used in the experiment. The angular position of the adapter in the *X*–*Y* plane can be determined by measuring the tilt angle (α) shown in Fig. 6. To perform the measurement, a special adapter with three coordinate arms was made using the 3-D printer, and it was attached to the wrist of each subject using elastic cloth, as also shown in Fig. 6. A weighted plumb string was used to define the global *Y* axis. A protractor was used to measure the a-angle. Then, the global transmissibility values at each frequency on the wrist in the *X* and *Y* directions ($T_{X\_Global–Wrist}$ and $T_{Y\_Global\_Wrist}$) are calculated using the following formulas [47]:

$$\begin{aligned} T_{X\_Global-Wrist} &= T_{X\_Local-Wrist}\cdot\cos(\alpha) - T_{Y\_Local-Wrist}\cdot\sin(\alpha) \\ T_{Y\_Global-Wrist} &= T_{X\_Local-Wrist}\cdot\sin(\alpha) + T_{Y\_Local-Wrist}\cdot\cos(\alpha) \end{aligned} \quad (5)$$

where $T_{X\_Local–Wrist}$ and $T_{Y\_Local–Wrist}$ are the local transmissibility measured with the adapter at the wrist in the *X* and *Y* directions, respectively.

2.6. Statistical analyses

Whenever applicable, the two repeated measures of wrist transmissibility under each condition were utilized for the statistical analyses. While it is well understood that the transmissibility is a function of vibration frequency, linear model analyses of variance (ANOVA) tests of vibration transmissibility were performed to identify the significance of the following fixed factors: measurement method (two levels: adapter and laser in both experiments), adapter type (three levels in the 3-D experiments and two levels in the 1-D experiments), and adapter tightness (two levels in the 3-D experiments only). Subject was treated as a random factor in all ANOVAs. The ANOVAs were performed using SPSS statistical software (IBM SPSS Statistics, version 16.0). Differences were considered significant at the $p < 0.05$ level.

3. Results

3.1. Evaluation of the adapter and 3-D laser vibrometer measurements

Fig. 7 shows the transmissibility spectra measured in the instrumentation check-up tests, in which the adapters were attached to the handle through foam. As expected, there are some differences among the transmissibility spectra of the adapters, as they have different masses, and the attachment tensions fastening them to the foam and handle may have varied slightly. However, the pair of spectra measured on a given adapter using the laser technology and the adapter method generally match well. The best match is found between their total vibration transmissibility spectra evaluated using Eq. (3), as shown in Fig. 7(a). Their differences are generally less than 7%, which is evaluated from the following formula: $|T_{Total\_Adapter} - T_{Total\_Laser}|/T_{Total\_Laser}$. This is because the total vibration transmissibility is theoretically independent of the coordinate system [45]. Fig. 7(a) also shows that the total transmissibility values measured with all the methods in the low-frequency range (<25 Hz) converge to unity. This is consistent with the basic theory of vibration response of a mechanical system. This further suggests that the measured data are reliable. Fig. 7(c) shows that the match and convergence to unity in the *Y* direction are also very good because it is relatively easier to align the adapter with the handle axial direction. However, in the *X* and *Z* directions, differences between the laser spectra and adapter spectra from the Adapter A checkup test are fairly large (>10%) at every frequency, as also shown in Fig. 7(b and d). The transmissibility value of Adapter A in the *X* direction measured using the adapter method is obviously greater than unity in the low-frequency range, but the value in the *Z* direction is underestimated by the same degree as the overestimation in the *X* direction. This is because it is difficult to fully align the coordinates of the adapter and handle [45].

3.2. Effects of the measurement method and adapter misalignment

Fig. 8 shows the comparisons of the mean transmissibility spectra of the subjects measured at the wrist using the 3-D laser vibrometer and Adapter A with medium attachment tightness. Similar to that observed in the instrumentation check-up tests shown in Fig. 7, the total vibration spectra measured on the adapter using both methods are very comparable in the entire frequency range of the experiment. The spectrum measured on the skin using the laser vibrometer is also generally consistent with that measured using the adapter. The statistical analysis also indicates that the measurement method is generally not a significant factor ($p > 0.79$). However, the frequency-stratified analysis confirms the significance of the difference between the laser-measured and adapter-measured spectra in most frequencies in the major resonant frequency range (12.5–40 Hz) of the wrist ($p < 0.05$). The maximum peak difference is 17.7%.

As also shown in Fig. 8, the laser-on-the-skin spectrum in each direction is comparable with the laser-on-the-adapter spectrum. However, the adapter-measured spectrum in each orthogonal direction was substantially different from those measured using the laser vibrometer, especially in the *X* and *Y* directions. As above-mentioned, such differences primarily result from the misalignment of the adapter relative to the global coordinates. With the hand–arm posture shown in Fig. 4, the average adapter tilt angle in the *X*–*Y* plane measured using the method shown in Fig. 6 is 31.5°. The local transmissibility spectra can

be transformed into the global transmissibility spectra using this angle with Eq. (5). The resulting spectra are plotted in Fig. 9, together with the laser-measured spectra. Obviously, the correction significantly improves the comparability.

3.3. Effect of the adapter mass

Fig. 10 shows the total transmissibility spectra measured at the wrist, forearm, and upper arm measured on the adapters under the medium attachment tightness. Again, the spectra measured with the two lightweight Adapters A (13 g) and B (15 g) using both technologies at each of the three measurement locations were comparable with each other and with those measured on the skin using the laser vibrometer. However, major differences were observed in the spectra measured using the heavier Adapter C (31 g) at the wrist; the critical resonant peak shifted from 25 Hz to 16 Hz, which is statistically significant ($p < 0.0002$).

3.4. Effect of the adapter attachment tightness

Fig. 11 shows the effect of adapter attachment tightness on the total vibration transmissibility measured at the wrist. Increasing the tightness increases the major resonant frequency of the adapter or shifts entire transmissibility spectrum of the adapter toward higher frequencies. For Adapters A and B, the increased tightness shifts the peak frequency from 25 Hz to 31.5 Hz, which creates a discrepancy with the laser-on-skin peak frequency (25 Hz). However, the first peak frequency for Adapter C (16 Hz) is shifted above 20 Hz, which is closer to the laser-on-skin peak frequency.

3.5. Results from 1-D experiments along the forearm direction

Fig. 12 shows the comparisons of the laser-measured and adapter-measured mean transmissibility spectra on the upper arms of the subjects along the forearm (Z) direction. There is no significant difference between the spectra measured using the two adapters (Adapters B and D) ($p = 0.57$), even though B is nearly twice the mass of D. However, their measured transmissibility spectra at frequencies below 16 Hz are obviously different from that measured using the laser vibrometer ($p < 0.001$). The magnitude of the transmissibility measured on the adapter using the adapter method is generally lower than that measured on the adapter using the laser vibrometer, but their phase angles are very similar, which indicates that the adapter was not fully aligned with the global Z direction or the upper arms of some subjects varied from 90° relative to the forearm direction during the measurement. The resonant peak magnitude of the laser-measured transmissibility on the upper arm skin is about 40% larger than that of the laser-measured transmissibility on the adapter. The phase angles are also substantially different at frequencies above 8 Hz. The resonant peak frequency varied with the subject in the range of 6.3–16 Hz with a median value of 10 Hz. The mean values of the resonant peak frequencies measured using laser-on-skin and laser-on-adapter (9.05 and 10.63 Hz, respectively) are suggestively different ($p < 0.073$).

Fig. 13(a) shows the comparisons of the transmissibility spectra measured on the upper arm and at the wrist along the forearm direction of a typical subject, their corresponding apparent mass measured at the palm of the hand, and the mechanical impedance (R_{Palm}) calculated from the apparent mass (M_{Palm}) using the following formula:

$$R_{Palm} = j\omega \cdot M_{Palm} \quad (6)$$

As shown in Fig. 13(a), the two major peak frequencies (10 and 25 Hz) observed in the wrist transmissibility spectrum occur at the same frequencies as those observed in the apparent mass or impedance. The peak transmissibility frequency (10 Hz) measured by the laser on the upper arm is also the same as the peak frequency of the apparent mass. While the adapter-measured peak frequency is obviously at a higher value (12.5 Hz) for this subject, the average increase across all six subjects is small or not significant, as reflected by the comparisons of the mean spectra shown in Fig. 13(b). Although the peaks of the mean response functions are smoothed out due to the averaging effects [48], the above-described correlations can still be observed in the mean spectra.

4. Discussion

Compared with directly attaching an accelerometer to the skin of the human body to measure the transmitted vibration, the use of an adapter for the attachment may have the following advantages:

I. The adapter can be designed to provide stable adaptation to the local contact geometry of each substructure, which can effectively reduce the rotational motions of the accelerometer in the measurement.

II. The edges of an accelerometer may be uncomfortable for the subject, especially during long-term measurement. This may be avoided by using an adapter. The larger adapter contact area can effectively distribute the overall contact pressure while maintaining sufficient contact stiffness in order to get reliable transmission of vibration from the local tissues to the accelerometer.

III. The adapter can make it easier to control the orientation of the accelerometer in the attachment for the measurement. The adapter can also serve as a platform for installing other electronic elements for data processing and wireless transmission.

IV. Although the adapter increases the attachment mass, the increased contact area can compensate for the effect of the increased mass.

The results of this study confirm that the adapter method is acceptable for some applications. This study also confirmed that the measurement of the transmissibility on the surface of the human arm is generally influenced by its attachment mass, tightness, and orientation, primarily because the attachment of the accelerometer may change the local dynamic properties of the hand–arm system, and thus its local responses. However, the results of this study also demonstrate that the influences are not as significant at some measurement locations when a lightweight adapter is used for the measurement. More importantly, this study provides useful information for understanding the influencing factors, which may help appropriately interpret and apply the measured transmissibility data.

4.1. Total vibration transmissibility versus directional vibration transmissibility

This study found that the misalignment of the local accelerometer coordinates relative to the global excitation coordinates is a significant source of error for the directional transmissibility measurements using the adapter method, as shown in Figs. 8 and 12. The measurement of the total vibration transmissibility avoids the misalignment issue [45]; hence, it is generally more reliable than the measurement of directional transmissibility using the adapter method, as also shown in Fig. 8. For this reason, this study used the total vibration transmissibility to examine the effects of the influencing factors on the transmissibility measurement. This finding also suggests that the total vibration transmissibility should be used in applications of vibration transmissibility whenever applicable. For example, the effectiveness of anti-vibration gloves can be more reliably assessed using the total vibration method [45]. The total vibration method is also consistent with the standard method for assessing the risk of hand-transmitted vibration exposures [26].

In this study's 1-D experiments, it was also observed that the total vibration transmissibility for a uniaxial excitation can be larger than the axial transmissibility. This is partially because some cross-axis vibration responses may also occur [49], especially in the low-frequency range (<25 Hz). This is also because the adapter accelerometer can only detect part of the vibration in the excitation direction if the adapter is not aligned with the input vibration direction. Therefore, the total vibration transmissibility may not be fully comparable with the directional transmissibility in the 1-D experimental study.

Besides the total vibration transmissibility, the directional vibration transmissibility is also required in some studies of hand-transmitted vibration exposures, as the detailed biodynamic responses and health effects may be direction-specific. Computer modeling of the hand–arm system also often requires the directional transmissibility. While it is possible to approximately align the axes in laboratory experiments, it is difficult to achieve the alignment at workplaces, as the tool orientations and arm postures may vary significantly during tool operations. This study demonstrated that the directional transmissibility can be obtained if the angles between the local coordinates of the accelerometer and the global coordinates of the excitation are measured, as shown in Fig. 9. This requires the development of a portable device that combines the measurements of the vibration and the coordinate angles, which may be considered in further studies.

4.2. Effects of adapter mass and attachment tightness

As revealed by the results of this study, while the adapter mass tends to reduce the resonant frequency of the local structure (Fig. 10), the force and constraint applied by the adapter and wrapping cloth tend to increase the natural frequency (Fig. 11). This is because increasing the structural mass reduces the natural frequency, but the applied pressure on the soft tissues underneath the adapter and elastic cloth increases the stiffness of the soft tissues and thus the natural frequency. These countervailing effects indicate that the adapter mass and tightness can be optimized such that their overall effect on the natural frequency can be minimized. As shown in Fig. 8, the adapter-measured resonant peak at the wrist is marginally higher than that measured with the laser vibrometer; however, the opposite phenomenon is observed in the transmissibility spectra measured on the upper arm, as shown in Fig. 12. The

sharper resonances of the laser on skin versus the laser on adapter and adapter measurements shown in Fig. 12 reveals the large damping influences of the elastic bands as well as the adapter mass effect. These observations also indicate that the adapter mass and attachment tightness effects are influenced by the thickness and dynamic properties of the soft tissue underneath the adapter and wrapping cloth. This also demonstrates how these effects are individual-specific.

Fortunately, the lightweight adapters do not substantially affect the measurement of the major natural frequencies of the human arms, as also shown in Figs. 8, 12 and 13. Although the magnitude and damping characteristics of the transmissibility may be significantly affected, the lightweight adapters do not change the basic trends of the transmissibility and its correlations with the driving-point response functions. As long as the transmissibility spectra are approximately correlated with the apparent mass or impedance spectra, the measured data may be considered acceptable, at least for an approximate understanding and simulation of the hand–arm system.

The results of this study suggest that the palm adapter recommended in the current ISO 10819 [43] is acceptable for the measurement of vibration transmissibility on the human arms. Further reducing the adapter weight from its limit (≤15 g) required in the standard may improve the measurement, but the benefit may not be substantial. As shown in Fig. 10, similar results are obtained using Adapter A (15 g) and Adapter B (13 g) at the wrist. The differences are also very small in the data measured on the upper arm using Adapter B and Adapter D (7 g) as shown in Fig. 12.

The results presented in Fig. 7 show that the percent differences between the spectra measured with the laser vibrometer and the adapter in the baseline test generally increase with frequency, especially for the phase. These observations suggest that the transmissibility spectra measured with these two technologies are comparable up to at least 315 Hz. This frequency range is adequate for measurements of human arm vibration.

The results of this study also suggest that it is neither necessary nor appropriate to tightly wrap the lightweight adapter on the arms if it is the soft tissue transmissibility that is of interest. For such a purpose, the tightness is acceptable as long as the tension is sufficient to secure the adapter without making the subject uncomfortable. If the purpose is to measure the bone transmissibility, it is naturally desired to select a bony location and to apply a tight attachment for the measurement. The adapter used in this study may not be suitable for the measurement at some bony locations. The exact effect of the attachment tightness on the measurement at such locations may also require further studies.

It should also be noted that some other adapters may also provide similar measurements. While the effects of the mass and tightness on the measurements observed in this study should be generally applicable, the wrapping force applied to each adapter may depend on the contact area of the adapters, as the contact pressure determines the contact stiffness. A unique benefit of using the standard adapter is that the results from different laboratories or studies can be compared if the standard adapter is consistently used in these studies.

4.3. The relationship between transmissibility and driving-point response function

The correlation between the peak transmissibility and the peak driving-point response function shown in Fig. 13 is consistent with that observed in some previous studies [50,51]. Such a correlation can be understood from the theorem derived by Dong et al. [20]. According to this theorem, the relationship between the apparent mass of the hand–arm system and the vibration transmissibility distributed throughout the system at each frequency can be expressed as follows:

$$\begin{aligned} M_{Fingers}+M_{Plam}=&\int_{Fingers}T(X,Y,Z)\cdot dm \\ &+\int_{Plam-wrist-forearm}T(X,Y,Z)\cdot dm \\ &+\int_{Upperarm-shoulder}T(X,Y,Z)\cdot dm \\ &+\int_{bodysubstructures}T(X,Y,Z)\cdot dm \end{aligned} \quad (7)$$

While the apparent mass measured at the fingers ($M_{Fingers}$) depends primarily on the responses distributed in the fingers ($\int_{Fingers} T(X, Y, Z)\cdot dm$), the apparent mass measured at the palm of the hand (M_{Palm}) depends primarily on the responses distributed in the palm-wrist-forearm, upper arm, and shoulder [13,18]. Therefore, the major resonant features of the vibration transmissibility should correlate with those of the apparent mass measured at the palm, as shown in Fig. 13.

4.4. Implications for modeling study

The results of this study demonstrate that the biodynamic responses on the arm and shoulder with the postures used in the experiments exhibit two major resonances. The first one is in the range of 6–12 Hz, with a mean value of about 10 Hz (Fig. 13(b)), which is primarily related to the responses of the upper arm and shoulder substructures. The second one is in the range of 16–40 Hz, with a mean value of 25 Hz (Fig. 13(b)), which is primarily related to the response of wrist-forearm substructures. These findings are similar to those reported before [13,17,18,24,34,37,51,52]. The finger responses were not measured in this study. Their fundamental resonance is usually in the range of 50–300 Hz, primarily depending on vibration direction, measurement location, and applied finger force [18,41,42,51]. These resonant features indicate that a model with at least three degrees of freedom (DOFs) is required to reasonably simulate the responses of the hand–arm system.

The model shown in Fig. 14 has three effective DOFs, and it meets the minimum requirement for the simulation. In addition to having a suitable model structure, according to Dong's theorem [20], the measured data should also be sufficiently accurate, and each transmissibility function should be sufficiently representative of the motion of its corresponding substructure(s) simulated as a lumped mass in the model to calibrate the model or to determine the model parameters. Otherwise, the modeling responses are unlikely to fit well with both apparent mass and transmissibility experimental data [28]. Therefore, the goodness of the curve fittings in the model calibration with both types of response functions can be used to assess the reliability and the appropriate representativeness of experimental data. As an example, the experimental data shown in Fig. 13(a), together the finger apparent mass reported in a previous study [51], were used to

calibrate the model. The comparisons of the curving fittings, together with the identified model parameters, are also shown in Fig. 14. The modeling responses generally fit the experimental data reasonably well, which suggests that the experimental data are acceptable, and the measured transmissibility spectra are approximately representative of the motions of their corresponding substructures.

As also expected, some differences between the modeling and experimental data can also be observed in Fig. 14. This is partially because it is impossible for a lumped-parameter model to fully represent the structural features of the complex hand–arm system. The transmissibility spectrum measured at a specific location on the skin surface of a substructure is generally not fully representative of the overall motion of the substructure simulated as a lumped mass in the model. Furthermore, some measurement errors are unavoidable, no matter which method is used in the measurement. If the purpose of the modeling study is to simulate the detailed responses using a comprehensive finite element model, the laser-measured data may be a better choice than the adapter-measured data for the model calibration or validation; such data are more representative of the local skin responses. If the purpose of the modeling study is to understand the basic characteristics of the responses and to roughly predict the distributed biodynamic responses using an efficient lumped-parameter model, the adapter-measured data may be sufficient. However, it should also be kept in mind that the adapter may marginally change the resonant frequency. The modeling driving-point response functions should match well with the experimental data, as they represent the integrated properties of the system, and they can be reliably measured using available technologies.

When both transmissibility and driving-point response functions are used in a model calibration, their relative weightings should be appropriately applied. Their baseline weightings can be defined based on the relationship equation of the model to be calibrated [28]. Equal relative weighting was applied in the calibration of the model shown in Fig. 14. However, for the above-mentioned reasons, it is recommended to apply more weighting to the apparent mass or mechanical impedance in the model calibration or parameter identification, especially when it is difficult to determine whether the measured transmissibility spectra are sufficiently accurate and/or representative.

5. Conclusions

This study examined an adapter method for measuring the skin surface vibration on the human arms. The results reveal that the magnitude and damping features of the adapter-measured transmissibility in major resonant frequency ranges are different from those of the laser-measured transmissibility, which suggests the adapter may affect the dynamic properties of the local structure. While increasing the adapter mass reduced the skin resonant frequency, increasing the tightness of the adapter attachment increased the resonant frequency. However, the use of lightweight (<15 g) adapters under medium attachment tightness did not change the basic shapes of the transmissibility spectra. These transmissibility magnitude spectra were also highly correlated with the apparent mass and were generally consistent with the modeling predictions, which suggest that the adapter-measured transmissibility spectra reflect the basic characteristics of the system responses.

Because the adapters may be significantly misaligned with the global coordinates of the vibration test systems, large errors were observed in the adapter-measured directional transmissibility. This study, however, also demonstrated that the misalignment issue can be resolved by using total vibration transmissibility or measuring the misalignment angles to correct the errors. Therefore, it is concluded that the adapter method is acceptable for understanding the basic characteristics of the vibration transmission in the human arms and for approximately modeling the system.

References

1. Griffin, MJ. Handbook of Human Vibration. Academic Press; London: 1990.
2. Pelmear, PL.; Wasserman, DE. Hand–Arm Vibration: A Comprehensive Guide for Occupational Health Professionals. OEM Press; Beverly Farms, MA, USA: 1998.
3. NIOSH. Musculoskeletal Disorders and Workplace Factors: A critical review of epidemiologic evidence for work-related musculoskeletal disorders of the neck, upper extremity, and low back. Cincinnati; OH, U.S: 1997. NIOSH Publication No. 97-141
4. Griffin MJ. Foundations of hand-transmitted vibration standards. Nagoya J Med Sci. 1994; 57(suppl):147–164. [PubMed: 7708097]
5. Pradko, F.; Lee, RA.; Greene, JD. Human vibration-response theory. Winter Annual Meeting of the Human Factors Division; Chicago. 7–11 November 1965; 65-WA/HUF-19, American Society of Mechanical Engineers
6. Cundiff JS. Energy dissipation in human hand–arm exposed to random vibration. J Acoust Soc Am. 1976; 59:212–214. [PubMed: 1249319]
7. Lidström, IM. Vibration injury in rock drillers, chiselers, and grinders. Some views on the relationship between the quantity of energy absorbed and the risk of occurrence of vibration injury; Proceedings of the 2nd International Conference on Hand–Arm Vibration; Cincinnati, OH, USA. 1977. p. 77-83.
8. Jen CJ, McIntire LV. Characteristics of shear-induced aggregation in whole blood. J Lab Clin Med. 1984; 103:115–124. [PubMed: 6690635]
9. Necking LE, Lundstrom R, Dahlin LB, Lundborg G, Thornell LE, Friden J. Tissue displacement is a causative factor in vibration-induced muscle injury. J Hand Surgery – Br Europ. 1996; 21B(6):753–757.
10. Wu JZ, Krajnak K, Welcome DE, Dong RG. Analysis of the dynamic strains in a fingertip exposed to vibration: correlation to the mechanical stimuli on mechanoreceptors. J Biomech. 2006; 39:2445–2456. [PubMed: 16168999]
11. Dong RG, Welcome DE, McDowell TW, Xu XS, Krajnak K, Wu JZ. A proposed theory on biodynamic frequency weighting for hand-transmitted vibration exposure. Ind Health. 2012; 50(5): 412–424. [PubMed: 23060254]
12. Suggs, CW. Modeling of the dynamic characteristic of hand–arm. In: Taylor, W., editor. The Vibration Syndrome. Academic Press; London: 1974. p. 169-186.
13. Dong JH, Dong RG, Rakheja S, Welcome DE, McDowell TW, Wu JZ. A method for analyzing absorbed power distribution in the hand and arm substructures when operating vibration tools. J Sound Vib. 2008; 311:1286–1304.
14. Wu JZ, Dong RG, Welcome DE, Xu XS. A method for analyzing vibration power absorption density in human fingertip. J Sound Vib. 2010; 329:5600–5614.
15. Reynolds DD, Falkenberg RJ. A study of hand vibration on chipping and grinding operators, Part I: Four-degree-of-freedom lumped parameter model of the vibration response of the human hand. J Sound Vib. 1984; 95:499–514.
16. Cherian T, Rakheja S, Bhat RB. An analytical investigation of an energy flow divider to attenuate hand-transmitted vibration. Int J Ind Ergon. 1996; 17:455–467.
17. Gurram R, Rakheja S, Brammer AJ. Driving-point mechanical impedance of the human hand–arm system: synthesis and model development. J Sound Vib. 1995; 180:437–458.

18. Dong RG, Dong JH, Wu JZ, Rakheja S. Modeling of biodynamic responses distributed at the fingers and the palm of the human hand–arm system. J Biomech. 2007; 40:2335–2340. [PubMed: 17166500]
19. Adewusi S, Rakheja S, Marcotte P. Biomechanical models of the human hand–arm to simulate distributed biodynamic responses for different postures. Int J Ind Ergon. 2012; 42:249–260.
20. Dong RG, Welcome DE, McDowell TW, Wu JZ. Theoretical relationship between vibration transmissibility and driving-point response functions of the human body. J Sound Vib. 2013; 332(24):6193–6202. [PubMed: 26663932]
21. ISO 2631-5, Mechanical Vibration and Shock—Evaluation of Human Exposure to Whole-body Vibration — Part 5: Methods for Evaluation of Vibration Containing Multiple Shocks. 2004
22. Thomas M, Beauchamp Y. Development of a new frequency weighting filter for the assessment of grinder exposure to wrist transmitted vibration. Comput Ind Eng. 1998; 35(3–4):651–654.
23. Dong RG, Welcome DE, Wu JZ. Frequency weightings based on biodynamics of fingers–hand–arm system. Ind Health. 2005; 43:485–494. [PubMed: 16100925]
24. Gurram R, Rakheja S, Gouw GJ. Vibration transmission characteristics of the human hand–arm system and gloves. Int J Ind Ergon. 1994; 13(3):217–234.
25. ISO 8727, Mechanical Vibration and Shock – Human Exposure – Biodynamic Coordinate Systems. 1997
26. ISO 5349-1, Mechanical Vibration – Measurement and Evaluation of Human Exposure to Hand-transmitted Vibration – Part 1: General Requirements. 2001
27. Freivalds, A. Biomechanics of the Upper Limbs – Mechanics, Modeling, and Musculoskeletal Injuries. CRC Press; New York: 2004.
28. Dong, RG.; Welcome, DE.; McDowell, TW.; Wu, JZ. Methods for calibrating human vibration models. Proceedings of the 5th American Conference on Human Vibration; Guelph, Ontario, Canada. 2014.
29. Pyykko I, Farkkila M, Toivanen J, Korhonen O, Hyvarinen J. Transmission of vibration in the hand–arm system with special reference to changes in compression and acceleration. Scand J Work Environ Health. 1976; 2:87–95. [PubMed: 959789]
30. Reynolds DD, Angevine EN. Hand–arm vibration. Part II: Vibration transmission characteristics of the hand and arm. J Sound Vib. 1977; 51:255–265.
31. Sakakibara H, Kondo T, Miyao M, Yamada S, Nakagawa T, Kobayashi F, Ono Y. Transmission of hand–arm vibration to the head, Scand. J Work Environ Health. 1986; 12:359–361.
32. Sörensson A, Lundström R. Transmission of vibration to the hand. J Low Freq Noise Vib. 1992; 11:14–22.
33. Aatola S. Transmission of vibration to the wrist and comparison of frequency response function estimators. J Sound Vib. 1989; 131:497–507.
34. Kihlberg S. Biodynamic response of the hand–arm system to vibration from an impact hammer and a grinder. Int J Ind Ergon. 1995; 16:1–8.
35. Kattel BP, Fernandez JE. The effect of rivet gun on hand–arm vibration. Int J Ind Ergon. 1999; 23:595–608.
36. Xu XS, Welcome DE, McDowell TW, Warren C, Dong RG. An investigation on characteristics of the vibration transmitted to wrist and elbow in the operation of impact wrenches. Int J Ind Ergon. 2009; 39:174–184.
37. Adewusi SA, Rakheja S, Marcotte P, Boutin J. Vibration transmissibility characteristics of the human hand–arm system under different postures, hand forces and excitation levels. J Sound Vib. 2010; 329:2953–2971.
38. Scalise L, Rossetti F, Paone N. Hand vibration: non-contact measurement of local transmissibility. Int Arch Occup Environ Health. 2007; 81:31–40. [PubMed: 17410375]
39. Rossi GL, Tomasini EP. Hand–arm vibration measurement by a laser scanning vibrometer. Measurement. 1995; 16(22):113–124.
40. Concettoni E, Griffin M. The apparent mass and mechanical impedance of the hand and the transmission of vibration to the fingers, hand, and arm. J Sound Vib. 2009; 325(3):664–678.

41. Welcome DE, Dong RG, Xu XS, Warren C, McDowell TW, Wu JZ. An investigation on the 3-D vibration transmissibility on the human hand–arm system using a 3-D scanning laser vibrometer. Can Acoust. 2011; 39(2):44–45.
42. Welcome DE, Dong RG, Xu XS, Warren C, McDowell TW. The effects of vibration-reducing gloves on finger vibration. Int J Ind Ergon. 2014; 44:45–59. [PubMed: 26543297]
43. ISO 10819, Mechanical Vibration and Shock. Method for the Measurement and Evaluation of the Vibration Transmissibility of Gloves at the Palm of the Hand. 1998
44. Dong, RG.; Welcome, DE.; McCormick, R. A novel 3-D hand–arm vibration test system and its preliminary evaluation. Proceedings of the 1st American Conference on Human Vibration; Morgantown, WV. June 2006;
45. Dong RG, Rakheja S, Smutz WP, Schopper AW, Wu JZ. Evaluating anti-vibration performance of a glove using total effective transmissibility. Int J Ind Ergon. 2002; 30:33–48.
46. Dong RG, Welcome DE, McDowell TW, Wu JZ. Measurement of biodynamic response of human hand–arm system. J Sound Vib. 2006; 294(4–5):807–827.
47. Kuipers, JB. Quaternions and Rotation Sequences. Princeton University Press; USA: 1999.
48. Dong RG, Welcome DE, McDowell TW, Wu JZ. Methods for deriving representative biodynamic response of hand–arm system to vibration. J Sound Vib. 2009; 325:1047–1061.
49. Rakheja, S.; Dong, RG.; Welcome, DE.; Ahmed, AKW. A preliminary study of cross-axis coupling effects in biodynamic response of the hand–arm system. Proceedings of the 11th International Conference on Hand–Arm Vibration; Bologna, Italy. 2007.
50. Xu XS, Welcome DE, McDowell TW, Wu JZ, Warren C, Dong RG. The vibration transmissibility and driving-point biodynamic response of the hand exposed to vibration normal to the palm, Int. J Ind Ergon. 2011; 41(5):418–427.
51. Dong RG, Welcome DE, McDowell TW, Wu JZ. Modeling of the biodynamic responses distributed at the fingers and palm of the hand in three orthogonal directions. J Sound Vib. 2013; 332:1125–1140. [PubMed: 26609187]
52. Kinne, J.; Latzel, K.; Schenk, TH. Application of two-hand impedance as basis for mechanical modeling. Proceedings of the 9th International Conference on Hand–Arm Vibration; Nancy, France. 2001. p. 113-118.

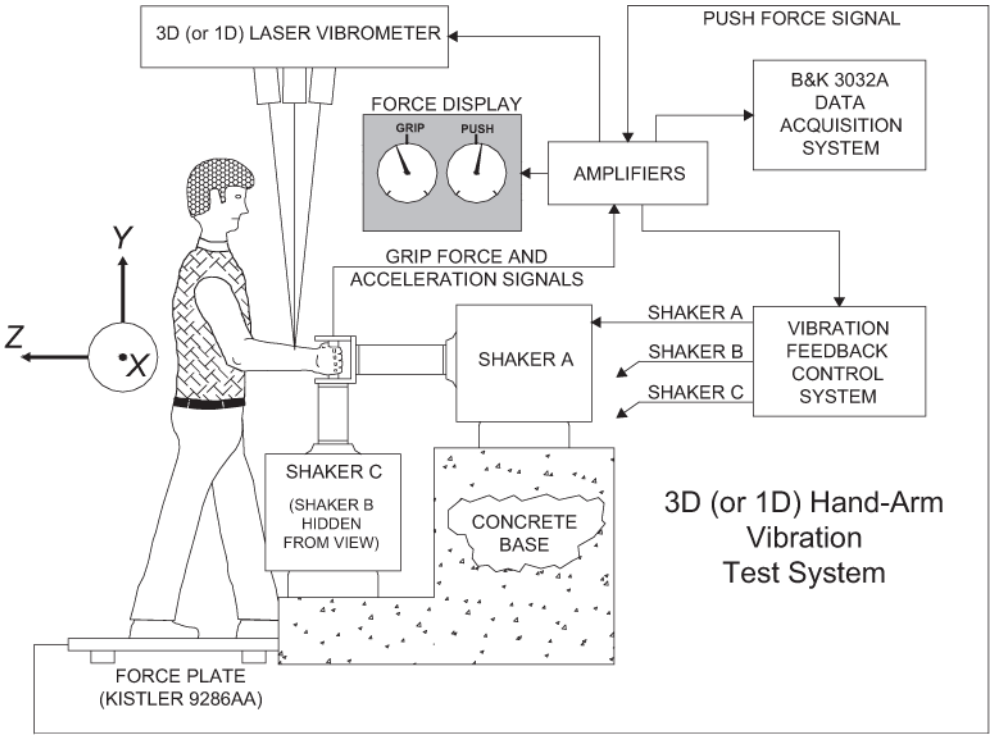

Fig. 1.

Subject and instrumentation setup that includes closed-loop controlled vibration excitation systems, 3-D and 1-D laser vibrometers, a vibration and response measurement system, and a grip force and push force measurement and display system.

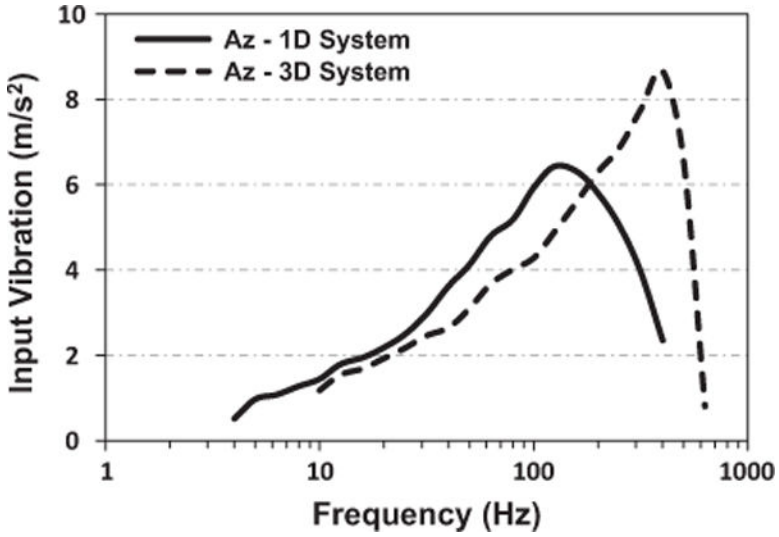

Fig. 2.
Input vibration spectra used on the 3-D and 1-D vibration test systems.

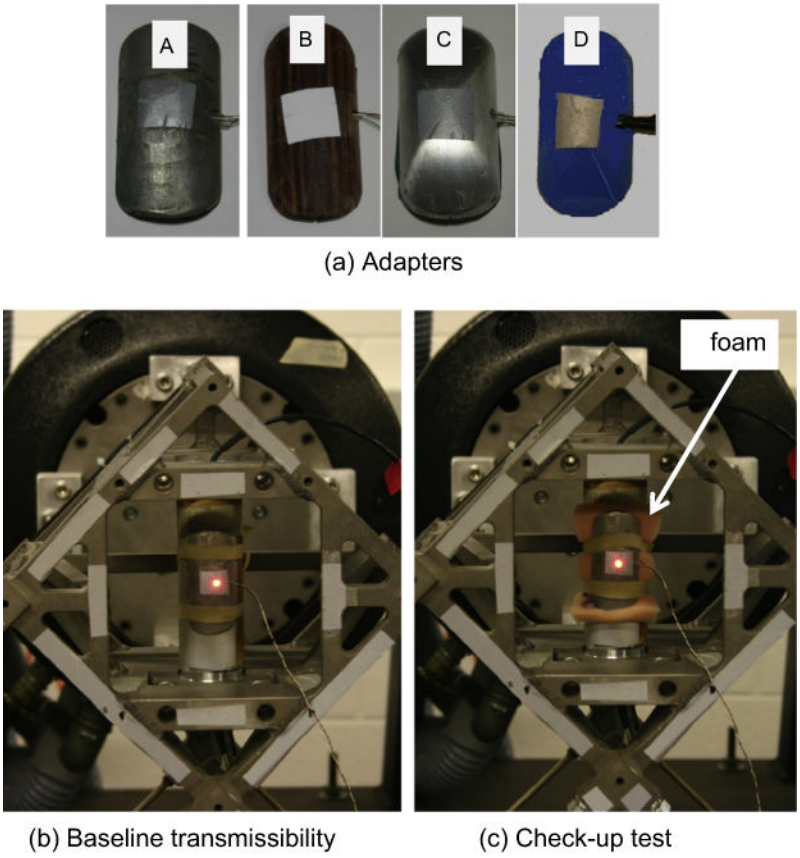

Fig. 3.

Four adapters (a) were used during the experiments. Adapter A was made of magnesium; Adapter B was made of wood; Adapter C was made of aluminum; and Adapter D was made of polylactic acid (PLA) using a 3-D printer. Adapters A, B, and C were used in the 3-D experiments while adapter B and D were used in the 1-D experiments. The calibration of the adapters on the 1-D and 3-D instrumented handles was done by measuring bare adapter transmissibility (b) and the adapter transmissibility on foam (c).

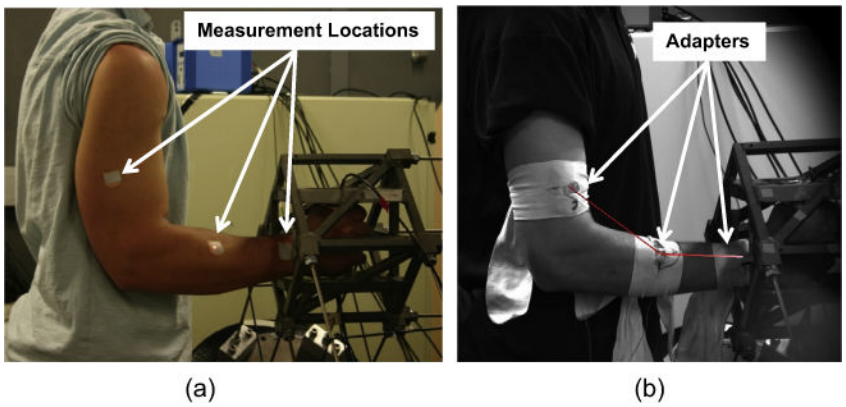

Fig. 4.

Pictorial views of the instrumentation setup on the 3-D vibration test system and a test subject with prescribed arm postures. (a) Retro-reflective tape was attached to the skin at the measuring points on the wrist and arm for laser-on-skin measurements. (b) Simultaneous measurements of vibration transmissibility were conducted using tri-axial accelerometer-equipped adapters and the 3-D laser vibrometer.

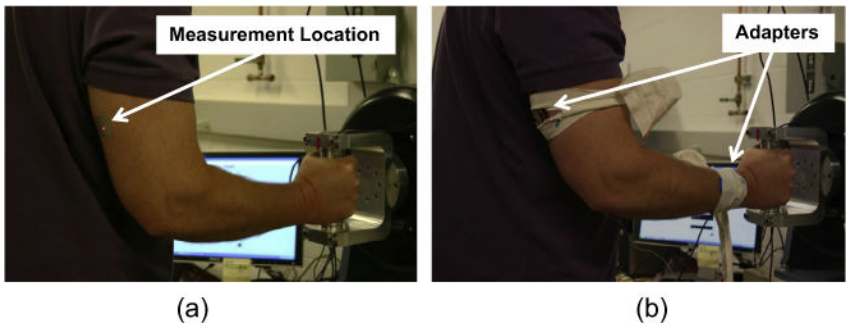

Fig. 5.

Pictorial views of the 1-D vibration test system and a test subject with instructed arm postures. (a) Retro-reflective tape was attached at the measurement point on the upper arm for laser-on-skin measurements. (b) Simultaneous measurements of vibration transmissibility to the wrist and upper arm were conducted with tri-axial accelerometer-equipped adapters and the 1-D laser vibrometer.

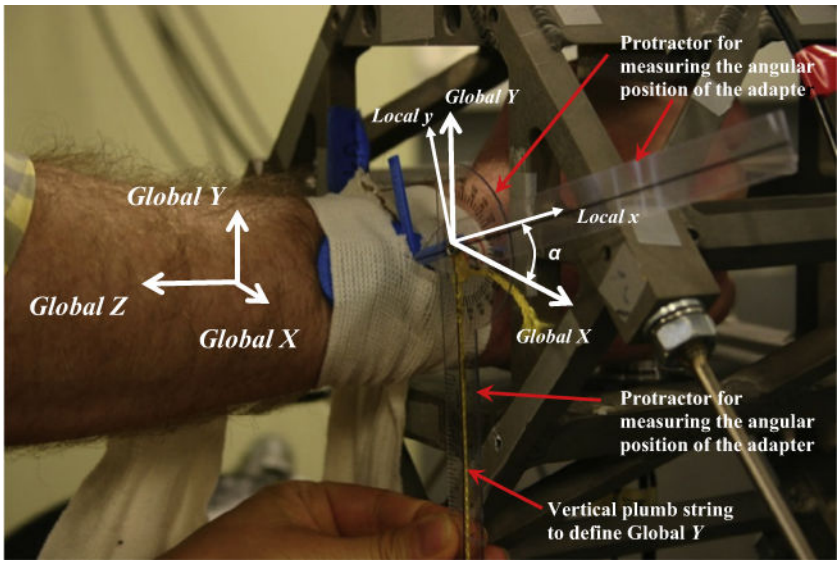

Fig. 6.
Adapter misalignment and correction.

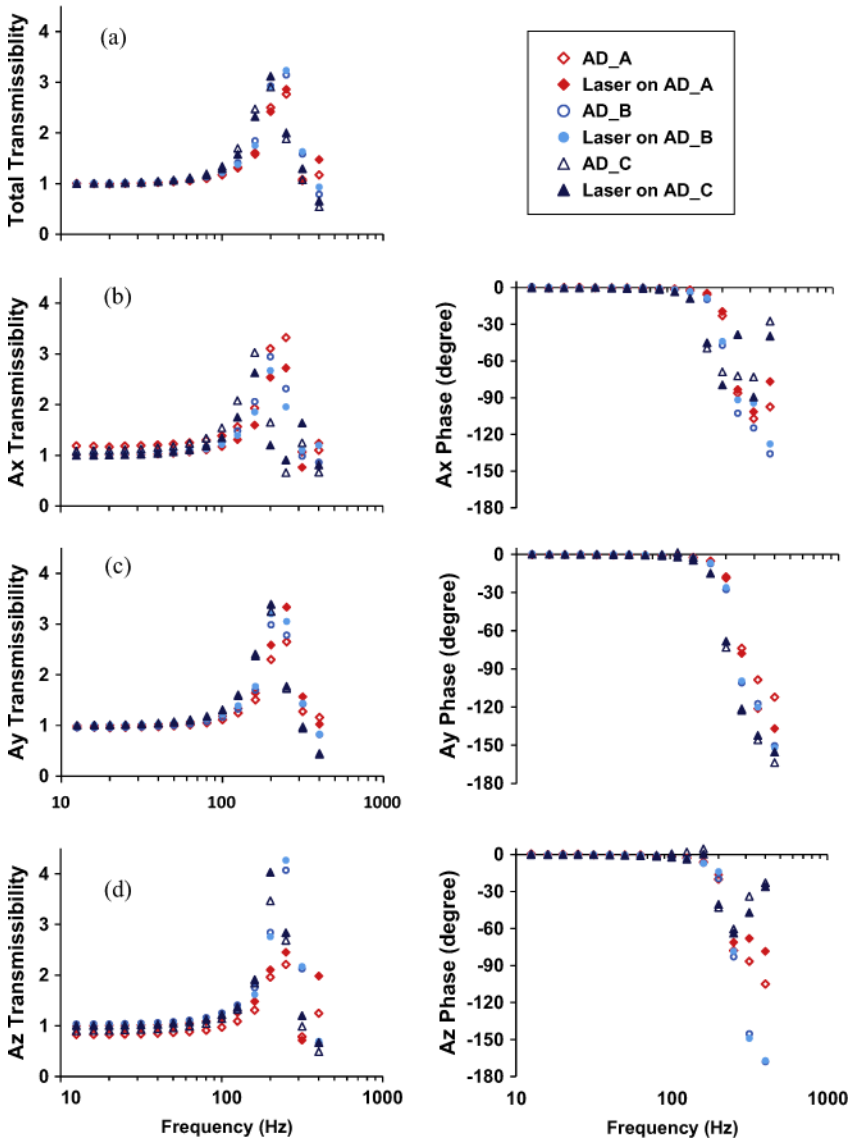

Fig. 7.
Vibration transmissibility of the adapters on 10 mm-thick foam on the instrumented handle.

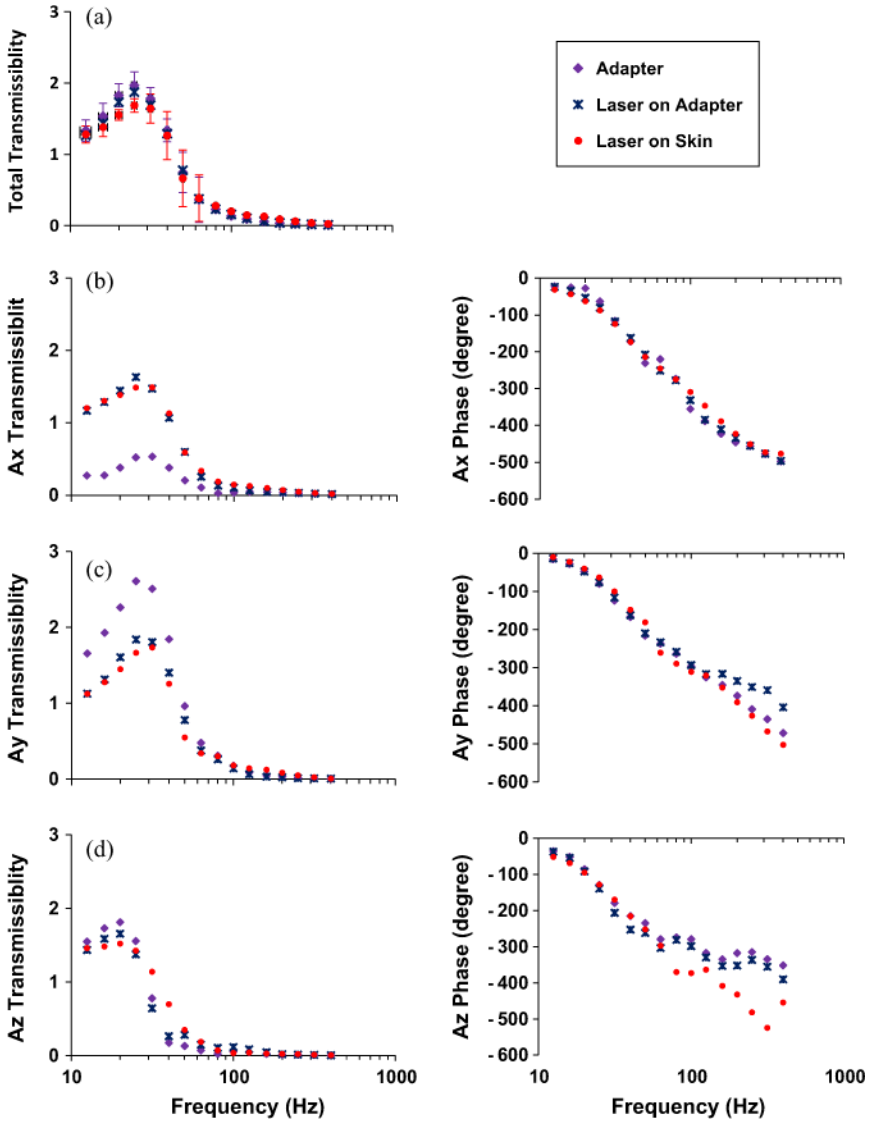

Fig. 8.

Averaged total and directional wrist vibration transmissibility spectra in global *X*, *Y*, and *Z* directions of the subjects measured by (1) adapter A with medium tightness attachment, and the laser vibrometer scanning (2) the surface of adapter and (3) the subject's skin.

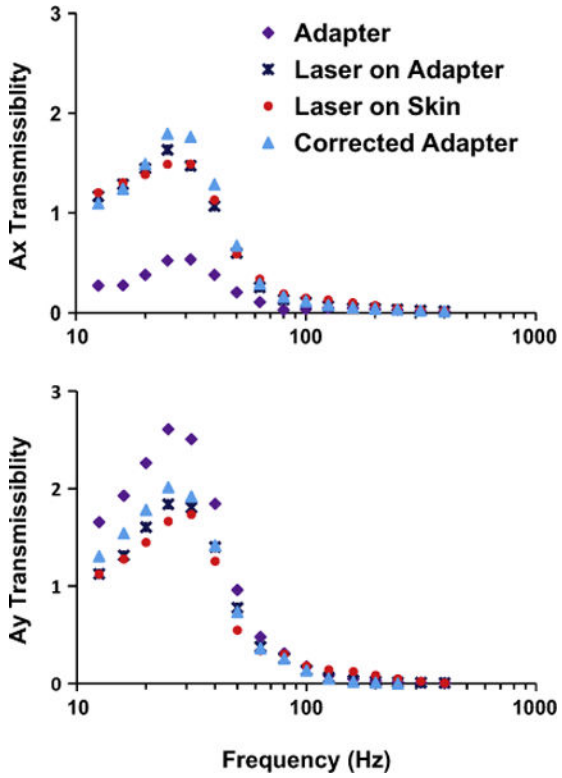

Fig. 9.
Results of the adapter misalignment correction.

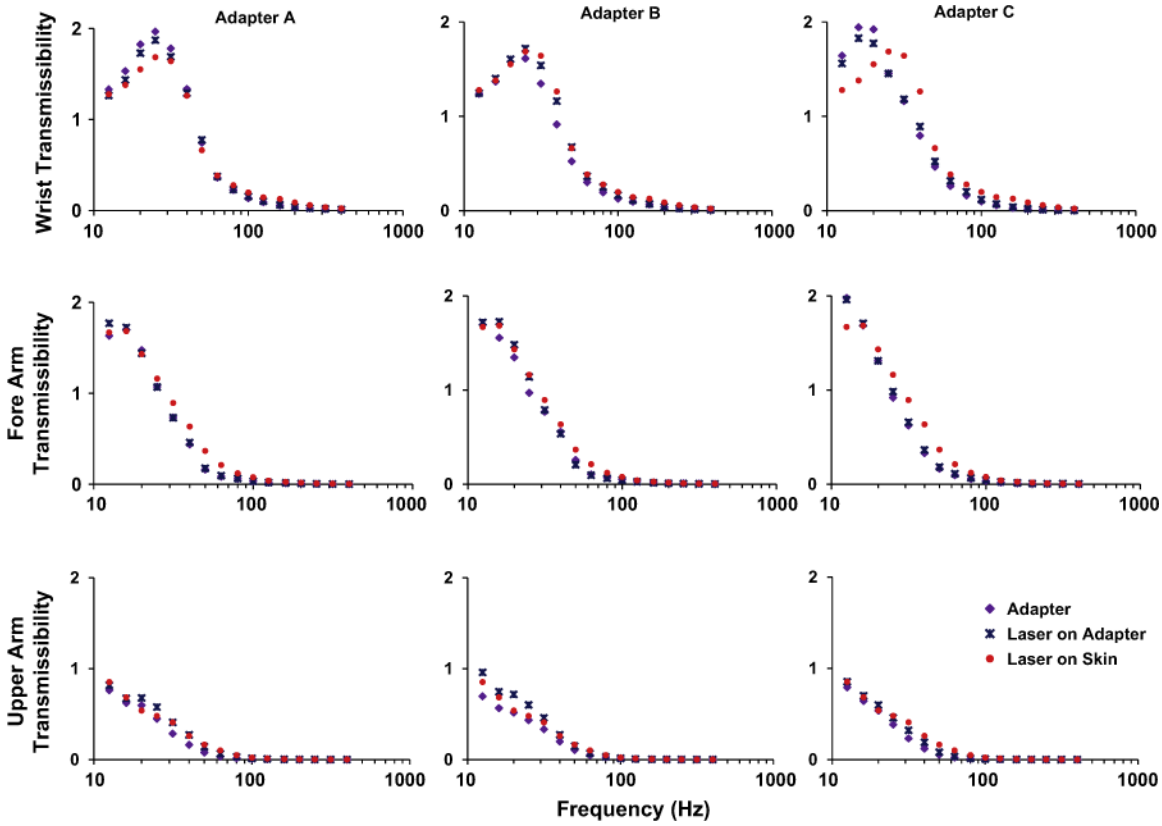

Fig. 10.

Averaged total vibration transmissibility of the subjects at the wrist, forearm, and upper arm measured by the adapters with medium tightness attachment, and the laser vibrometer scanning the surfaces of the adapter and the subject's skin.

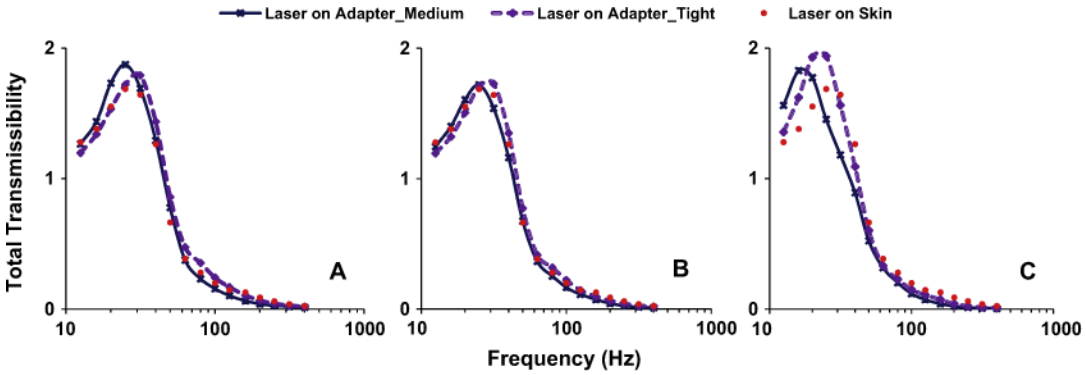

Fig. 11.

Averaged total vibration transmissibility of the subjects at the wrist, measured with the laser vibrometer scanning the surfaces of the subject's skin and the adapters with different levels of attachment tightness.

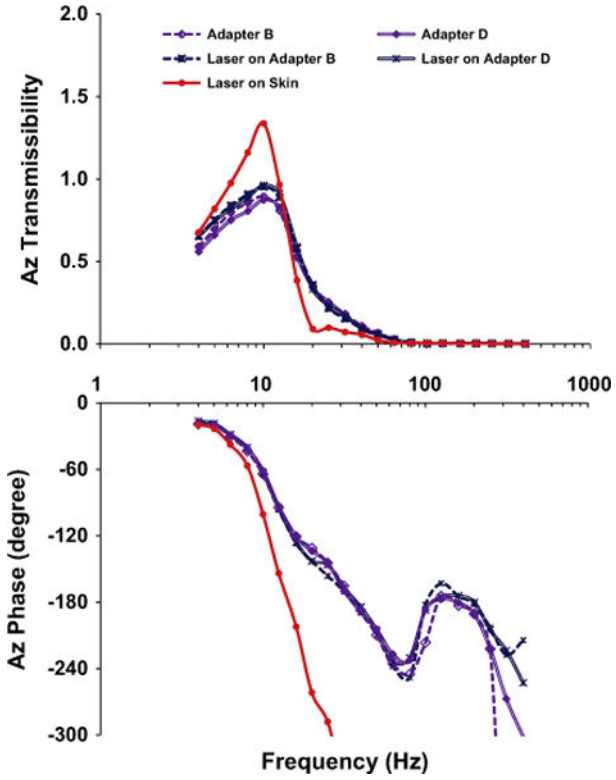

Fig. 12.

Comparisons of the upper arm vibration transmissibility spectra measured using the laser vibrometer and adapter methods.

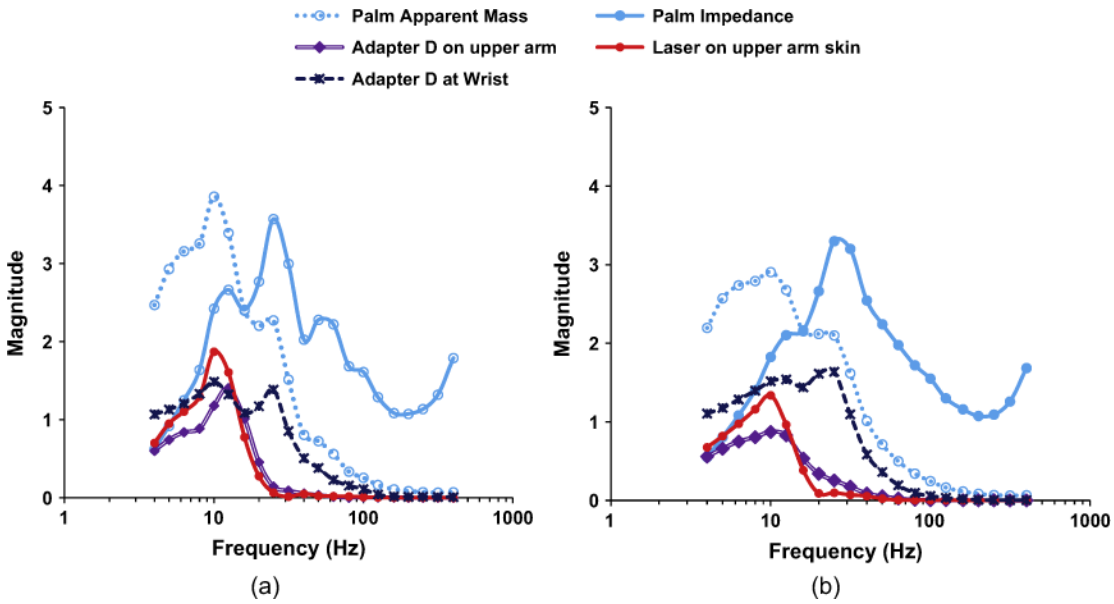

Fig. 13.

Correlations of the transmissibility, apparent mass, and mechanical impedance from: (a) the spectra measured with a typical subject; (b) the mean spectra of six subjects.

M_1	0.072	kg	$k3$	36835	N/m
M_2	2.371	kg	$k4$	99900	N/m
M_3	1.991	kg	$c0$	86	N-s/m
M_{01}	0.016	kg	$c1$	54	N-s/m
M_{02}	0.030	kg	$c2$	29	N-s/m
$k0$	2332	N/m	$c3$	100	N-s/m
$k1$	12352	N/m	$c4$	72	N-s/m
$k2$	3305	N/m			

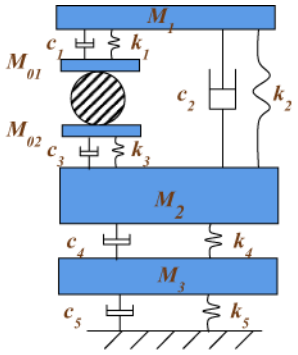

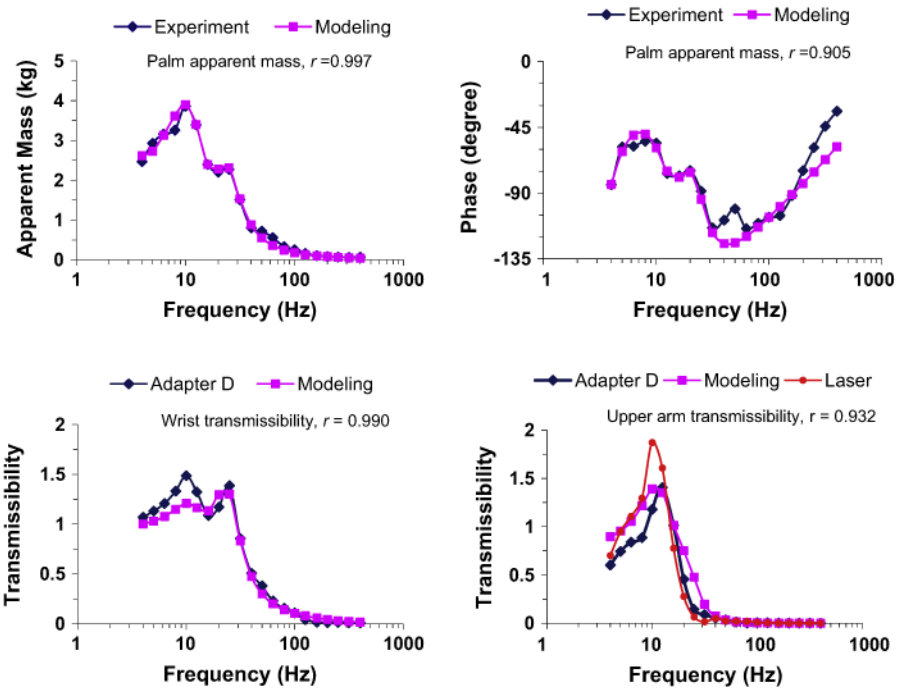

Fig. 14.

A model of the hand–arm system and the comparisons of the modeling results with the experimental data.

Table 1

Anthropometry data of the subjects in the 3-D and the 1-D vibration experiments (hand length = tip of middle finger to crease at wrist; hand breadth = the width measured at metacarpal).

Subject	3-D vibration test				1-D vibration test			
	Height (cm)	Weight (kg)	Hand length (mm)	Hand breadth (mm)	Height (cm)	Weight (kg)	Hand length (mm)	Hand breadth (mm)
1	182.9	84.6	198	90	181.6	83.3	208	94
2	190.5	78.1	199	85	182.2	85.5	194	90
3	182.2	95.7	197	94	182.2	93.6	198	94
4	180.3	82.2	199	90	180.3	84.2	199	90
5	182.9	101.3	197	93	182.9	101.3	197	93
6	169.0	65.0	175	77	175.3	81.0	195	84
Mean	181.3	84.5	194	88	180.8	88.1	199	91
SD	7.0	12.9	9.4	6.3	2.8	7.8	5.0	3.8

Measurement (Lond). Author manuscript; available in PMC 2016 January 29.